Equilibration timescale of atmospheric secondary organic aerosol partitioning

Manabu Shiraiwa[1] and John H. Seinfeld[1]

Received 25 September 2012; revised 30 October 2012; accepted 6 November 2012; published 18 December 2012.

[1] Secondary organic aerosol (SOA) formed from partitioning of oxidation products of anthropogenic and biogenic volatile organic compounds (VOCs) accounts for a substantial portion of atmospheric particulate matter. In describing SOA formation, it is generally assumed that VOC oxidation products rapidly adopt gas-aerosol equilibrium. Here we estimate the equilibration timescale, τ_{eq}, of SOA gas-particle partitioning using a state-of-the-art kinetic flux model. τ_{eq} is found to be of order seconds to minutes for partitioning of relatively high volatility organic compounds into liquid particles, thereby adhering to equilibrium gas-particle partitioning. However, τ_{eq} increases to hours or days for organic aerosol associated with semi-solid particles, low volatility, large particle size, and low mass loadings. Instantaneous equilibrium partitioning may lead to substantial overestimation of particle mass concentration and underestimation of gas-phase concentration. **Citation:** Shiraiwa, M., and J. H. Seinfeld (2012), Equilibration timescale of atmospheric secondary organic aerosol partitioning, *Geophys. Res. Lett.*, *39*, L24801, doi:10.1029/2012GL054008.

1. Introduction

[2] Organic aerosol is ubiquitous in the atmosphere [*Goldstein and Galbally*, 2007; *Zhang et al.*, 2007]. The major component of OA is secondary organic aerosol (SOA), the formation of which involves the multi-generation gas-phase oxidation of volatile organic compounds (VOCs), leading to an array of lower volatility oxidation products that partition between the gas and condensed phases [*Jimenez et al.*, 2009; *Kroll and Seinfeld*, 2008]. The aerosol condensed phase is generally a mixture of organic and inorganic compounds, such as sulfate, nitrate, ammonium, and water. It is generally assumed that the semi-volatile organic oxidation products rapidly establish a gas-particle equilibrium partitioning [*Odum et al.*, 1996; *Donahue et al.*, 2006]. The theory upon which the equilibrium partitioning is based relies on the implicit assumption that the condensed phase is homogeneously mixed.

[3] Recent evidence has emerged of the existence of semi-solid SOA [*Virtanen et al.*, 2010; *Saukko et al.*, 2012]. Glass transition temperatures of α-pinene related SOA compounds range over 260–310 K [*Koop et al.*, 2011]. It has been found that α-pinene secondary organic aerosol does not evaporate in a thermodenuder as predicted by equilibrium partitioning theory [*Cappa and Wilson*, 2011], and unexpectedly slow evaporation of ambient and laboratory-generated α-pinene SOA has also been observed [*Vaden et al.*, 2011]. *Perraud et al.* [2012] observed non-equilibrium formation and growth of α-pinene SOA, consistent with semi-solid behavior. Conceptually, it has been shown that the aerosol phase state, as characterized by its viscosity or bulk diffusivity, can assume liquid, semi-solid, or glassy solid state depending on ambient relative humidity (RH) and temperature [*Koop et al.*, 2011; *Mikhailov et al.*, 2009; *Shiraiwa et al.*, 2011].

[4] Given these observations of aerosol phase states, an overriding question is the effect of this phase state on the common assumption of gas-particle partitioning equilibrium, specifically the effect of mass transport in the bulk of amorphous semi-solid particles. The present work provides a theoretical analysis of the equilibration timescale of SOA partitioning in liquid, semi-solid, and amorphous solid particles using the kinetic flux model KM-GAP [*Shiraiwa et al.*, 2012a] (see auxiliary material), which resolves mass transport in both gas and particle phases.[1] The model allows a systematic evaluation of the equilibration timescale as a function of SOA volatility, bulk-phase diffusivity, surface accommodation coefficient, and particle size.

[5] In the present study we evaluate numerically the time to establish gas-particle equilibrium for a large range of SOA parameters. While the results for any numerical simulation strictly reflect only the conditions of that simulation, by varying volatility and aerosol phase state over a wide range it is possible to infer general conclusions concerning the establishment of gas-particle equilibrium and how the rate depends on the key properties of the SOA system. While data sets indicating the existence of semi-solid aerosol phases are emerging, it is not yet possible to link the type of detailed simulations that we present here to specific experiments due to the shortage of measurements of SOA viscosity. Nonetheless, we are able to anticipate from the numerical simulations the effect of SOA volatility and aerosol phase state on the nature of the SOA growth that will occur.

2. Gas-Particle Partitioning

[6] The volatility of a compound i can be expressed by the effective saturation mass concentration $C_i^* = 10^6\, M_i p_i^o/760\, RT$, where M_i (g mol^{-1}) is the molecular weight of compound i, p_i^o (Torr) is the saturation vapor pressure of pure compound i, R (m^3 atm mol^{-1} K^{-1}) is the gas constant, and

[1]Division of Chemistry and Chemical Engineering, California Institute of Technology, Pasadena, California, USA.

Corresponding author: J. H. Seinfeld, Division of Chemistry and Chemical Engineering, California Institute of Technology, 1200 E. California Blvd., Pasadena, CA 91125, USA. (seinfeld@caltech.edu)

0094-8276/12/2012GL054008

[1]Auxiliary materials are available in the HTML. doi:10.1029/2012GL054008.

Table 1. Properties and Kinetic Parameters of the Oxidation Product VOC Used in the Simulations for SOA Growth

Parameter (Unit)	Description	Values
$\alpha_{s,0}$	surface accommodation coefficient on free-substrate[a]	1
τ_d (s)	desorption lifetime [see *Shiraiwa et al.*, 2012a]	10^{-9}
ρ (g cm^{-3})	density	1.0
D_b (cm^2 s^{-1})	bulk diffusion coefficient[b]	10^{-8}
D_g (cm^2 s^{-1})	gas-phase diffusion coefficient	0.1
k_g (min^{-1})	first-order rate coefficient of conversion for VOC → SVOC	0.1
M (g mol^{-1})	molar mass	100

[a] $\alpha_{s,0}$ is varied for determining the effect of surface accommodation.
[b] D_b is varied for representing the effect of particle phase state.

T (K) is temperature. Note that ideal mixing condition is considered for simplicity. At gas-particle equilibrium, $p_i = p_{s,i}$, namely $C_i^g = C_i^s$, where p_i and C_i^g are the partial pressure and mass concentration in the vapor phase, respectively, and $p_{s,i}$ and C_i^s are the partial pressure and mass concentration of i just above the particle surface, respectively. Note that $p_{s,i}$ obeys Raoult's law in equilibrium with the near-surface bulk, which is resolved by KM-GAP. At $p_{s,i} < p_i$ ($C_i^s < C_i^g$), species i will diffuse from the gas to the particulate phase (diffusion-limited growth). If p_i changes slowly and $p_{s,i}$ follows p_i instantaneously ($p_{s,i} \approx p_i$), the particle still grows (quasi-equilibrium growth). The equilibration timescale τ_{eq} can be defined as the e-folding time for relaxation of the partial pressure gradient.

[7] We illustrate the evaluation of τ_{eq} for condensation of a semi-volatile compound generated by oxidation of a

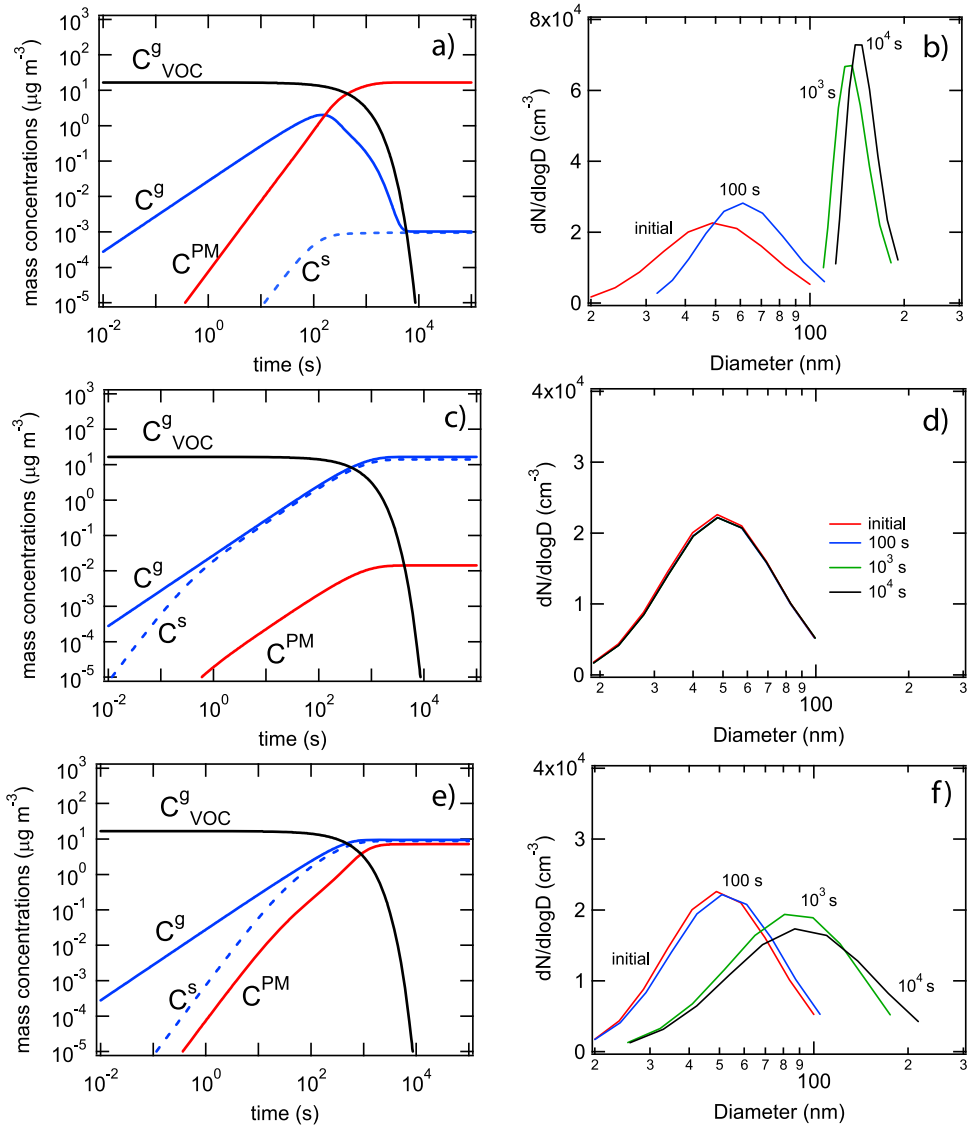

Figure 1. Temporal evolution of mass concentration of the VOC oxidation product in the gas phase (C^g; blue), just above particle surface (C^s; dashed blue), and in the particulate matter phase (C^{PM}; red) with (a) LVOC ($C^* = 10^{-3}$ μg m^{-3}), (c) IVOC ($C^* = 10^3$ μg m^{-3}), and (e) SVOC ($C^* = 10$ μg m^{-3}) for liquid particles. The gas-phase mass concentration of the parent VOC (C^g_{VOC}) is shown by the black line. The temporal evolution of the size distribution is shown for (b) LVOC, (d) IVOC, and (f) SVOC.

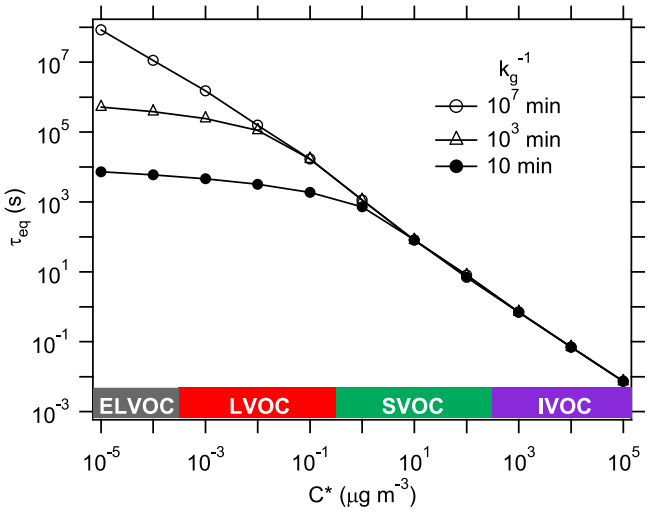

Figure 2. Equilibration timescales of SOA partitioning (τ_{eq}) for liquid particles as function of effective saturation concentration (C^*) with different first-order production rates of SVOC (k_g) of 10^{-7} min^{-1} (open circle), 10^{-3} min^{-1} (triangle), and 10^{-1} min^{-1} (solid circle). SOA growth is limited by gas-phase diffusion for low volatility VOC ($C^* < 10$ μg m^{-3}), whereas it is governed by quasi-equilibrium for high volatility VOC ($C^* > 10$ μg m^{-3}).

parent VOC. We assume that the parent VOC, with an initial concentration of 10^{11} cm^{-3}, is converted to the semi-volatile product with a given first-order rate coefficient, k_g. Conversion of this first-generation product to higher generation compounds need not be considered. The physical and kinetic parameters assumed for the system are given in Table 1. To investigate the effect of volatility of the oxidation product on τ_{eq}, C^* is varied over the range of 10^{-5}–10^5 μg m^{-3}. The initial number and mass concentrations of non-volatile pre-existing particles are taken as 10^4 cm^{-3} and 1 μg m^{-3}, respectively. The initial particle size distribution is assumed log-normal with mean diameter $D_{mean} = 50$ nm and standard deviation $\sigma = 1.5$. The nominal aerosol-phase bulk diffusion coefficient (D_b) is assumed to be 10^{-8} cm^2 s^{-1}, corresponding to that of a viscous-liquid droplet [*Koop et al.*, 2011], and the surface accommodation coefficient $\alpha_{s,0} = 1$ (the fraction of impinging molecules that are adsorbed at the particle surface). Note that surface tension is set to be 0.04 N m^{-1} and the use of different values within the range of 0.02–0.07 N m^{-1} gives practically the same results.

[8] In the nominal simulation of a very low volatility product ($C^* = 10^{-3}$ μg m^{-3}), gas-particle equilibrium is reached at $\sim 10^4$ s (Figure 1a). Particle growth is controlled by gas-phase diffusion because $C^g > C^s$ in the course of the particle growth. The evolution of the particle size distribution exhibits the narrowing characteristic of diffusion-limited particle growth [*Seinfeld and Pandis*, 2006; *Zhang et al.*, 2012] (Figure 1b). In the case of an intermediate volatility oxidation product ($C^* = 10^3$ μg m^{-3}), the gas-phase partial pressure gradient vanishes within $\sim$1 s, and as the mass concentration of the product in the gas phase, C^g, continues to increase due to the conversion of the parent VOC, the mass concentration of the product just above the particle surface, C^s, tracks the change in C^g essentially instantaneously (Figure 1c). In this case, the gas-phase rate of formation of the oxidation product controls particle growth (so-called quasi-equilibrium growth). Due to the relatively high volatility assumed for the condensing species, the particle grows only slightly (Figure 1d).

[9] Figure 1e shows the comparable results for a semi-volatile oxidation product ($C^* = 10$ μg m^{-3}). Particle growth is initially governed by gas-phase diffusion until $\sim 10^2$ s. After this initial period, the peak of the size distribution increases with increasing width (Figure 1f), which is characteristic of quasi-equilibrium growth. The larger particles absorb more vapor thus grow preferentially, as the equilibrium vapor pressure over their surface is smaller than that over smaller particles due to the Kelvin effect [*Zhang et al.*, 2012].

[10] Figure 2 shows τ_{eq} as a function of C^*. τ_{eq} increases as C^* decreases, as the partial pressure gradient between the gas phase and the particle surface is larger for smaller C^* [*Meng and Seinfeld*, 1996; *Marcolli et al.*, 2004; *Zhang et al.*, 2012]. The effects of reaction rate constant k_g are investigated by varying k_g in the range of 0.1–10^{-7} min^{-1}. τ_{eq} is independent of k_g as long as $\tau_{eq} < k_g^{-1}$. The slope of τ_{eq} decreases when $\tau_{eq} > k_g^{-1}$, because the rate of formation of the oxidation product drops due to consumption of the parent VOC that would otherwise increase linearly. τ_{eq} of ELVOC and LVOC is of order hours, and their growth may be governed by gas-phase diffusion, while τ_{eq} of SVOC and IVOC is the order of seconds, thus controlled by quasi-equilibrium growth. τ_{eq} can be regarded as the timescale for transition from kinetically-limited growth to quasi-equilibrium growth.

[11] To examine the influence on τ_{eq} of surface accommodation coefficient $\alpha_{s,0}$ and particle phase state, as reflected by the bulk diffusivity D_b, we consider, for convenience, the growth of mono-disperse particles of initial diameter 200 nm from a condensing oxidation product of $C^* = 10$ μg m^{-3}. The initial gas-phase VOC concentration is 10^{11} cm^{-3} and initial particle number concentration is 10^4 cm^{-3}. In calculation of τ_{eq}, $\alpha_{s,0}$ and D_b are varied over the ranges of 10^{-3} -1 and 10^{-21}–10^{-5} cm^2 s^{-1}, respectively. Note that typical values of D_b of organics are 10^{-10}–10^{-5} cm^2 s^{-1} for liquid, 10^{-20}–10^{-10} cm^2 s^{-1} for semi-solid, and $<10^{-20}$ cm^2 s^{-1} for solid [*Shiraiwa et al.*, 2011].

[12] The value of $\alpha_{s,0}$ has a major impact on τ_{eq} for liquid and semi-solid particles with relatively high D_b (Figure 3). Decrease of $\alpha_{s,0}$ by an order of magnitude leads to roughly an order of magnitude increase in τ_{eq} SOA growth is limited by gas-phase diffusion at $\alpha_{s,0} \approx 1$, but becomes limited by surface accommodation at smaller $\alpha_{s,0}$. In this $\alpha_{s,0}$ - limited regime, τ_{eq} is insensitive to D_b because surface-bulk exchange and bulk diffusion are more rapid than surface accommodation. When D_b decreases below a certain threshold, the timescales for surface-bulk exchange and bulk diffusion become longer than that of gas-phase diffusion and accommodation. In this case, τ_{eq} is insensitive to $\alpha_{s,0}$ but sensitive to D_b. In the D_b - limited regime, decrease of D_b by an order of magnitude leads to roughly an order of magnitude increase in τ_{eq}; for the conditions of the simulation, τ_{eq} is the order of minutes for semi-solid particles with $D_b \approx 10^{-15}$ cm^2 s^{-1}, increasing to days and longer for particles with $D_b < 10^{-20}$ cm^2 s^{-1}.

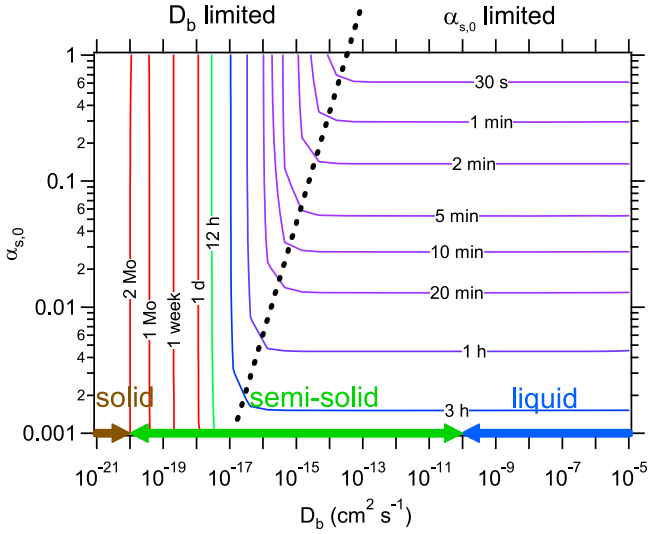

Figure 3. Equilibration timescale τ_{eq} of partitioning of SVOC (C^* = 10 μg m^{-3}) in liquid, semi-solid, and solid particles as functions of surface accommodation coefficient ($\alpha_{s,0}$) and bulk diffusion coefficient (D_b).

[13] We investigate the impact on τ_{eq} of size and concentration of pre-existing particles, over the range of 30–1000 nm and 0.1–100 μg m^{-3}, respectively (Figure 4). Initial conditions are the same as those of the prior calculation with $\alpha_{s,0}$ = 1 and C^* = 10 μg m^{-3}. The growth of monodisperse particles is considered. Figure 4 shows τ_{eq} for viscous liquid (D_b = 10^{-8} cm^{-3}) and semi-solid (D_b = 10^{-15} cm^{-3}) particles. A larger diameter leads to longer τ_{eq}: for example, at a typical ambient concentration of 1 μg m^{-3}, τ_{eq} is on the order of minutes for 100 nm liquid particles, increasing to the order of hours for 1 μm particles (Figure 4a). In this comparison ambient particle mass concentration is held constant, so increasing particle size translates to a decrease of the number and surface area concentration of particles, and a decrease of total accommodation of molecules to the surface. An increase of particle concentration also leads to an increase of surface area concentration, thereby leading to a decrease of τ_{eq} Note that all particles are assumed to be spherical in our analysis; if SOA particles are non-spherical with a larger surface area, τ_{eq} would be correspondingly smaller.

[14] Typical SOA mass concentrations in laboratory chamber experiments lie in the range of 10–100 μg m^{-3}. Over this range, τ_{eq} for accumulation mode particles is on the order of minutes for both liquid and semi-solid particles. Therefore, SOA particles formed at these mass loadings will be in gas-particle equilibrium. Typical ambient organic mass concentrations in Beijing [*Sun et al.*, 2010], Mexico City [*Jimenez et al.*, 2009], Los Angeles Basin [*Hersey et al.*, 2011], Hyytiälä, Finland [*Raatikainen et al.*, 2010], and Amazon Basin [*Chen et al.*, 2009] are indicated in Figure 4. With the exception of highly polluted urban areas such as Beijing and Mexico City, ambient organic mass concentrations are typically <10 μg m^{-3}, and τ_{eq} is of order minutes for liquid particles and hours or more for semi-solid particles. The time required to reach equilibrium is sufficiently long such that atmospheric SOA constituents may exist in a non-equilibrium state, particularly for semi-solid aerosol particles.

3. Kinetic Versus Instantaneous Partitioning

[15] To evaluate the common assumption of instantaneous gas-particle partitioning and investigate the impact of kinetic effects on predicted mass concentrations in gas and particulate phases, here we compare the comprehensive results of the kinetic flux model to those of an equilibrium gas-particle partitioning model. The evolution of mass concentration is represented by condensation of semi-volatile VOC generated by oxidation of a parent VOC with the same conditions as in Figure 1 and Table 1. In the instantaneous gas-particle partitioning model, the VOC oxidation product instantaneously partitions into the particle phase, and gas-phase and bulk diffusion kinetics are ignored.

[16] For IVOC (C^* = 10^3 μg m^{-3}), both models give almost identical results, because SOA growth is governed by the quasi-equilibrium growth mechanism (Figure S1a). For LVOC, however, the instantaneous partitioning model overestimates the particle phase concentration by an order of magnitude and underestimates the gas-phase concentration up to several orders of magnitude before equilibration is established (Figure S1b). For partitioning of SVOC (C^* = 10 μg m^{-3}) into semi-solid particles (D_b =

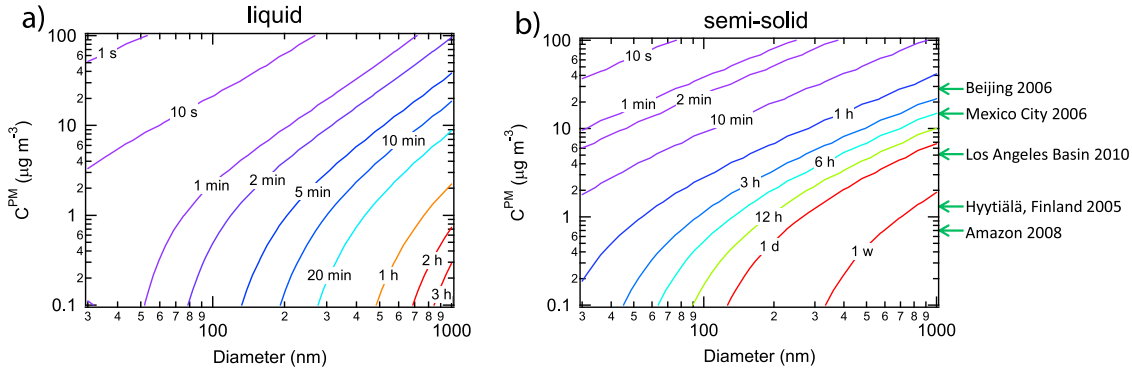

Figure 4. Equilibration timescale of SOA partitioning τ_{eq} of SVOC (C^* = 10 μg m^{-3}) in (a) liquid (D_b = 10^{-8} cm^{-3}) and (b) semi-solid (D_b = 10^{-15} cm^{-3}) as functions of particle diameter (nm) and mass concentration of pre-existing particles (μg m^{-3}). Ambient organic mass concentrations are indicated.

10^{-15} cm^{-3}), the assumption of instantaneous equilibrium overestimates the particle phase concentration by one order of magnitude (Figure S1c). These results clearly establish the validity of instantaneous gas-particle partitioning for relatively high volatility compounds partitioning into liquid particles, but this assumption breaks downs for partitioning of low and semi-volatile compounds into liquid and semi-solid particles, leading to overestimation of the particle phase concentration and underestimation of the gas-phase concentration.

4. Discussion

[17] It has been reported that the growth of freshly-nucleated particles is governed by kinetically-limited growth rather than quasi-equilibrium growth [*Riipinen et al.*, 2011]. Indeed, the evolution of the size distribution in nucleation events often shows the narrowing characteristic of diffusion-limited growth. An apparent C^* of ultrafine particles is estimated to be 10^{-3}–10^{-2} $\mu g\ m^{-3}$ [*Pierce et al.*, 2011; *Brock et al.*, 2011], resulting in an equilibration timescale of hours. Such low-volatility compounds may be generated by chemical reactions in the condensed phase in addition to gas-phase formation with subsequent condensation [*Kalberer et al.*, 2004; *Ervens et al.*, 2011; *Riipinen et al.*, 2012]. The formation of oligomers and other multifunctional organic substances with high molecular mass and low vapor pressure is one mechanism that could lead to solidification, resulting in an increase of particle viscosity and decrease of bulk diffusivity [*Pfrang et al.*, 2011; *Koop et al.*, 2011], which could significantly affect the condensation and evaporation kinetics. The evolution of the particle phase due to reactive uptake and condensed phase chemistry and phase change in the course of particle growth are not included in this study.

[18] Slow equilibration conditions are more likely to be prevalent in remote areas with low aerosol mass concentrations, for example, in boreal forests, where SOA has been found to exhibit amorphous solid behavior [*Virtanen et al.*, 2010], and in the mid and upper troposphere, where SOA most likely undergoes a glass transition [*Zobrist et al.*, 2008; *Koop et al.*, 2011]. Moreover, slow equilibration may be more relevant under flow tube conditions with reaction times of minutes than for chamber studies with considerably longer time scales. In addition to SOA growth, the results obtained in this study are directly applicable to SOA evaporation. Several studies have observed unusually slow evaporation of ambient and laboratory-generated SOA [*Grieshop et al.*, 2007; *Vaden et al.*, 2011]. These observations are consistent with the evaporation timescale of semi-solid SOA, as shown in Figures 3 and 4b. Note that slow evaporation may be also due to highly complex multi-component mixtures with high molecular mass and low vapor pressure [*Widmann et al.*, 1998]. Such slow evaporation timescales can potentially affect volatility measurements using a thermodenuder, in which organics may not be in a glassy state but remain highly viscous [*Riipinen et al.*, 2010; *Cappa and Wilson*, 2011; *Saleh et al.*, 2011].

[19] The results obtained here have direct implications on hygroscopic growth and activation kinetics of cloud condensation nuclei, as the presence of a semi-solid state can inhibit diffusion of water in the bulk [*Mikhailov et al.*, 2009; *Zobrist et al.*, 2011; *Tong et al.*, 2011; *Raatikainen et al.*, 2012; *Bones et al.*, 2012]. Moreover, reactive uptake of trace species such as OH, O_3 and NO_3 is also influenced by slow bulk diffusion of oxidants [*Shiraiwa et al.*, 2011, 2012b]. The occurrence of a semi-solid state and resulting kinetic effects may requires a more detailed representation of SOA formation than presently available.

[20] **Acknowledgments.** This work was supported by National Science Foundation grant AGS-1057183. MS is supported by the Japan Society for the Promotion of Science (JSPS) Postdoctoral Fellowship for Research Abroad. The authors thank Andreas Zuend, Xi Zhang and Ulrich Pöschl for helpful discussions.

[21] The Editor thanks two anonymous reviewers for their assistance in evaluating this paper.

References

Bones, D. L., et al. (2012), Comparing the mechanism of water condensation and evaporation in glassy aerosol, *Proc. Natl. Acad. Sci. U. S. A.*, *109*(29), 11,613–11,618, doi:10.1073/pnas.1200691109.

Brock, C. A., D. M. Murphy, R. Bahreini, and A. M. Middlebrook (2011), Formation and growth of organic aerosols downwind of the Deepwater Horizon oil spill, *Geophys. Res. Lett.*, *38*, L17805, doi:10.1029/2011GL048541.

Cappa, C. D., and K. R. Wilson (2011), Evolution of organic aerosol mass spectra upon heating: Implications for OA phase and partitioning behavior, *Atmos. Chem. Phys.*, *11*(5), 1895–1911, doi:10.5194/acp-11-1895-2011.

Chen, Q., et al. (2009), Mass spectral characterization of submicron biogenic organic particles in the Amazon Basin, *Geophys. Res. Lett.*, *36*, L20806, doi:10.1029/2009GL039880.

Donahue, N. M., et al. (2006), Coupled partitioning, dilution, and chemical aging of semivolatile organics, *Environ. Sci. Technol.*, *40*(8), 2635–2643, doi:10.1021/es052297c.

Ervens, B., B. J. Turpin, and R. J. Weber (2011), Secondary organic aerosol formation in cloud droplets and aqueous particles (aqSOA): A review of laboratory, field and model studies, *Atmos. Chem. Phys.*, *11*(21), 11,069–11,102, doi:10.5194/acp-11-11069-2011.

Goldstein, A. H., and I. E. Galbally (2007), Known and unexplored organic constituents in the Earth's atmosphere, *Environ. Sci. Technol.*, *41*(5), 1514–1521, doi:10.1021/es072476p.

Grieshop, A. P., N. M. Donahue, and A. L. Robinson (2007), Is the gas-particle partitioning in alpha-pinene secondary organic aerosol reversible?, *Geophys. Res. Lett.*, *34*, L14810, doi:10.1029/2007GL029987.

Hersey, S. P., et al. (2011), The Pasadena Aerosol Characterization Observatory (PACO): Chemical and physical analysis of the western Los Angeles basin aerosol, *Atmos. Chem. Phys.*, *11*(15), 7417–7443, doi:10.5194/acp-11-7417-2011.

Jimenez, J. L., et al. (2009), Evolution of organic aerosols in the atmosphere, *Science*, *326*(5959), 1525–1529, doi:10.1126/science.1180353.

Kalberer, M., et al. (2004), Identification of polymers as a major components of atmospheric organic aerosols, *Science*, *303*(5664), 1659–1662, doi:10.1126/science.1092185.

Koop, T., et al. (2011), Glass transition and phase state of organic compounds: Dependency on molecular properties and implications for secondary organic aerosols in the atmosphere, *Phys. Chem. Chem. Phys.*, *13*(43), 19,238–19,255, doi:10.1039/c1cp22617g.

Kroll, J. H., and J. H. Seinfeld (2008), Chemistry of secondary organic aerosol: Formation and evolution of low-volatility organics in the atmosphere, *Atmos. Environ.*, *42*(16), 3593–3624, doi:10.1016/j.atmosenv.2008.01.003.

Marcolli, C., et al. (2004), Internal mixing of the organic aerosol by gas phase diffusion of semivolatile organic compounds, *Atmos. Chem. Phys.*, *4*, 2593–2599, doi:10.5194/acp-4-2593-2004.

Meng, Z. Y., and J. H. Seinfeld (1996), Time scales to achieve atmosphere gas-aerosol equilibrium for volatile species, *Atmos. Environ.*, *30*(16), 2889–2900, doi:10.1016/1352-2310(95)00493-9.

Mikhailov, E., et al. (2009), Amorphous and crystalline aerosol particles interacting with water vapor: Conceptual framework and experimental evidence for restructuring, phase transitions and kinetic limitations, *Atmos. Chem. Phys.*, *9*(24), 9491–9522, doi:10.5194/acp-9-9491-2009.

Odum, J. R., et al. (1996), Gas/particle partitioning and secondary organic aerosol yields, *Environ. Sci. Technol.*, *30*(8), 2580–2585, doi:10.1021/es950943+.

Perraud, V., et al. (2012), Nonequilibrium atmospheric secondary organic aerosol formation and growth, *Proc. Natl. Acad. Sci. U. S. A.*, *109*(8), 2836–2841, doi:10.1073/pnas.1119909109.

Pfrang, C., M. Shiraiwa, and U. Pöschl (2011), Chemical ageing and transformation of diffusivity in semi-solid multi-component organic aerosol

particles, *Atmos. Chem. Phys.*, *11*(14), 7343–7354, doi:10.5194/acp-11-7343-2011.

Pierce, J. R., et al. (2011), Quantification of the volatility of secondary organic compounds in ultrafine particles during nucleation events, *Atmos. Chem. Phys.*, *11*(17), 9019–9036, doi:10.5194/acp-11-9019-2011.

Raatikainen, T., et al. (2010), Physicochemical properties and origin of organic groups detected in boreal forest using an aerosol mass spectrometer, *Atmos. Chem. Phys.*, *10*(4), 2063–2077, doi:10.5194/acp-10-2063-2010.

Raatikainen, T., et al. (2012), A coupled observation—Modeling approach for studying activation kinetics from measurements of CCN activity, *Atmos. Chem. Phys.*, *12*(9), 4227–4243, doi:10.5194/acp-12-4227-2012.

Riipinen, I., et al. (2010), Equilibration time scales of organic aerosol inside thermodenuders: Evaporation kinetics versus thermodynamics, *Atmos. Environ.*, *44*(5), 597–607, doi:10.1016/j.atmosenv.2009.11.022.

Riipinen, I., et al. (2011), Organic condensation: A vital link connecting aerosol formation to cloud condensation nuclei (CCN) concentrations, *Atmos. Chem. Phys.*, *11*(8), 3865–3878, doi:10.5194/acp-11-3865-2011.

Riipinen, I., et al. (2012), The contribution of organics to atmospheric nanoparticle growth, *Nat. Geosci.*, *5*(7), 453–458, doi:10.1038/ngeo1499.

Saleh, R., A. Shihadeh, and A. Khlystov (2011), On transport phenomena and equilibration time scales in thermodenuders, *Atmos. Meas. Tech.*, *4*(3), 571–581, doi:10.5194/amt-4-571-2011.

Saukko, E., et al. (2012), Humidity-dependent phase state of SOA particles from biogenic and anthropogenic precursors, *Atmos. Chem. Phys.*, *12*(16), 7517–7529, doi:10.5194/acp-12-7517-2012.

Seinfeld, J. H., and S. N. Pandis (2006), *Atmospheric Chemistry and Physics: From Air Pollution to Climate Change*, 2nd ed., John Wiley, New York, doi:10.1063/1.882420.

Shiraiwa, M., et al. (2011), Gas uptake and chemical aging of semisolid organic aerosol particles, *Proc. Natl. Acad. Sci. U. S. A.*, *108*(27), 11,003–11,008, doi:10.1073/pnas.1103045108.

Shiraiwa, M., et al. (2012a), Kinetic multi-layer model of gas-particle interactions in aerosols and clouds (KM-GAP): Linking condensation, evaporation and chemical reactions of organics, oxidants and water, *Atmos. Chem. Phys.*, *12*(5), 2777–2794, doi:10.5194/acp-12-2777-2012.

Shiraiwa, M., U. Pöschl, and D. A. Knopf (2012b), Multiphase chemical kinetics of NO_3 radicals reacting with organic aerosol components from biomass burning, *Environ. Sci. Technol.*, *46*(12), 6630–6636, doi:10.1021/es300677a.

Sun, J., et al. (2010), Highly time- and size-resolved characterization of submicron aerosol particles in Beijing using an Aerodyne Aerosol Mass Spectrometer, *Atmos. Environ.*, *44*(1), 131–140, doi:10.1016/j.atmosenv.2009.03.020.

Tong, H. J., et al. (2011), Measurements of the timescales for the mass transfer of water in glassy aerosol at low relative humidity and ambient temperature, *Atmos. Chem. Phys.*, *11*(10), 4739–4754, doi:10.5194/acp-11-4739-2011.

Vaden, T. D., et al. (2011), Evaporation kinetics and phase of laboratory and ambient secondary organic aerosol, *Proc. Natl. Acad. Sci. U. S. A.*, *108*(6), 2190–2195, doi:10.1073/pnas.1013391108.

Virtanen, A., et al. (2010), An amorphous solid state of biogenic secondary organic aerosol particles, *Nature*, *467*, 824–827, doi:10.1038/nature09455.

Widmann, J. F., C. M. Heusmann, and E. J. Davis (1998), The effect of a polymeric additive on the evaporation of organic aerocolloidal droplets, *Colloid Polym. Sci.*, *276*(3), 197–205, doi:10.1007/s003960050229.

Zhang, Q., et al. (2007), Ubiquity and dominance of oxygenated species in organic aerosols in anthropogenically-influenced Northern Hemisphere midlatitudes, *Geophys. Res. Lett.*, *34*, L13801, doi:10.1029/2007GL029979.

Zhang, X., S. N. Pandis, and J. H. Seinfeld (2012), Diffusion-limited versus quasi-equilibrium aerosol growth, *Aerosol Sci. Technol.*, *46*(8), 874–885, doi:10.1080/02786826.2012.679344.

Zobrist, B., et al. (2008), Do atmospheric aerosols form glasses?, *Atmos. Chem. Phys.*, *8*(17), 5221–5244, doi:10.5194/acp-8-5221-2008.

Zobrist, B., et al. (2011), Ultra-slow water diffusion in aqueous sucrose glasses, *Phys. Chem. Chem. Phys.*, *13*, 3514–3526, doi:10.1039/c0cp01273d.